Dynamical Buildup of a Quantized Hall Response from Nontopological States

Ying Hu,[1] Peter Zoller,[1,2] and Jan Carl Budich[1,2]

[1]*Institute for Quantum Optics and Quantum Information of the Austrian Academy of Sciences, 6020 Innsbruck, Austria*
[2]*Institute for Theoretical Physics, University of Innsbruck, 6020 Innsbruck, Austria*

We consider a two-dimensional system initialized in a topologically trivial state before its Hamiltonian is ramped through a phase transition into a Chern insulator regime. This scenario is motivated by current experiments with ultracold atomic gases aimed at realizing time-dependent dynamics in topological insulators. Our main findings are twofold. First, considering coherent dynamics, the nonequilibrium Hall response is found to approach a topologically quantized time-averaged value in the limit of slow but nonadiabatic parameter ramps, even though the Chern number of the state remains trivial. Second, adding dephasing, the destruction of quantum coherence is found to stabilize this Hall response, while the Chern number generically becomes undefined. We provide a geometric picture of this phenomenology in terms of the time-dependent Berry curvature.

Introduction.—Exploring the unique properties of topological insulators [1,2] such as Chern insulators [3] has become a major focus of research in physics. At zero temperature, the direct correspondence between the Chern number of the ground state, the Hall conductance, and the chiral edge states is well established [4,5]. By contrast, far from thermal equilibrium the topological properties of the time-dependent Hamiltonian and the state may not concur [6–10], and their relation to natural observables is a subject of ongoing open discussion [11–17]. Yet, such nonequilibrium scenarios generically occur in present experiments on ultracold gases [18–26], where starting from a topologically trivial initial state, the Hamiltonian is driven into a topological parameter regime, thus going through a topological quantum phase transition [cf. Fig. 1(a)]. However, the Chern number of the state is well known to remain zero under coherent dynamics. This topological discrepancy between the actual state versus the Hamiltonian immediately raises the challenge as to which manifestations of topology can be observed, even without entering a Chern insulator state, i.e., without adiabatically following the ground state. Below, we report two major theoretical contributions to address this issue, which may also shed light on ongoing experiments aimed at observing quantum Hall physics with cold atoms.

First we show that the nonequilibrium bulk Hall response can be quantized—at least in an asymptotic sense—reflecting uniquely the topology of the instantaneous Hamiltonian, despite the nontopological nature of the state at all times. Our main result on the coherent dynamics is shown in Fig. 1(b): a nonequilibrium Hall response exhibiting strongly oscillatory behavior in time is found to build up when the Hamiltonian enters a Chern insulator regime. The time-averaged Hall response at large times approaches a topologically quantized value in the limit of

slow but nonadiabatic ramps. Second, we find that adding classical noise induced dephasing not only stabilizes this Hall response [see Fig. 1(c)] but also allows for a geometric interpretation that eludes the standard notion of Chern numbers in closed systems (see Figs. 2 and 3). The central entity underlying this picture is the time-dependent Berry curvature of the density matrix describing the mixed state of the open system. In particular, we find that the Berry curvature generically acquires discontinuities [see Figs. 2(d) and 3(d)] that render the Chern number not well defined. This is found to originate from the interplay of the Landau-Zener (LZ) dynamics [31] around the gap closing and dephasing without energy relaxation. These observations allow us to explain the behavior of the Hall response, including its dependence on the ramp velocity and asymptotic quantization. While recent studies have focused on the coherent dynamics of chiral edge states [9,10], our present theoretical findings reveal a conclusive picture of bulk response properties in nonequilibrium Chern insulators beyond the coherent framework.

Topological discrepancy: Hamiltonian versus state.— As a paradigmatic example [32] of a Chern insulator [3] exhibiting quantum Hall physics, we consider a time-dependent lattice version of the massive 2D Dirac Hamiltonian [33]

$$H(m(t)) = \sum_k c_k^\dagger H_k(m(t)) c_k = \sum_k c_k^\dagger [\vec{d}_k(m(t)) \cdot \vec{\sigma}] c_k.$$

(1)

Here, c_k denotes the two-spinor of fermionic operators at lattice momentum k, and $\vec{d}_k(m(t)) = (\sin(k_x), \sin(k_y), m(t) + \cos(k_x) + \cos(k_y))$, where energy is measured in units of the hopping strength. For fixed m, the lower band
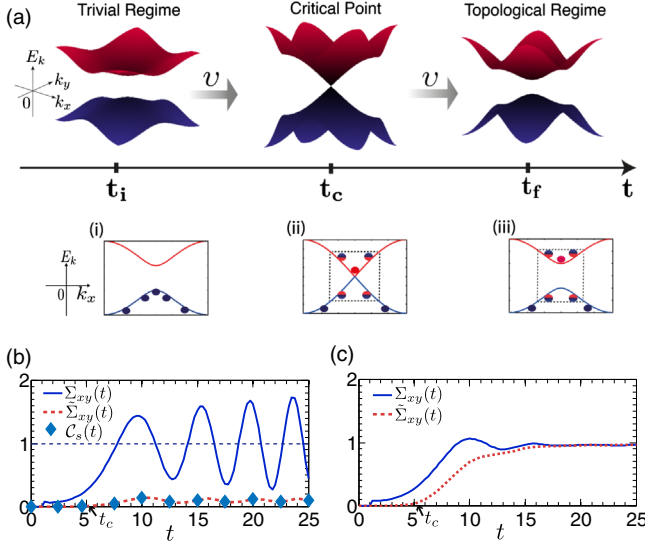
FIG. 1. (a) Parameter ramp in the system Hamiltonian from the nontopological to the topological regime through a phase transition. The insets show cuts of the band structure along the k_x axis ($k_y = 0$), illustrating (i) the initial state, (ii) the creation of excitations near the energy gap closing point, and (iii) the nonequilibrium state after the transition. (b),(c) Nonequilibrium Hall response $\Sigma_{xy}(t)$ [see Eq. (4)] and quasistatic ansatz $\tilde{\Sigma}_{xy}(t)$ [see Eq. (5)], with (b) coherent and (c) dephasing dynamics for the dephasing rate $\gamma_k = 0.15$, for the ramp $m(t) = m_i + (m_f - m_i)[1 - \exp(-vt)]$, $m_i = -2.7$, $m_f = -1.0$, $v = 0.1$ of the Hamiltonian (1). In (b), $\mathcal{C}_s$ of the pure state [see Eq. (2)] trivially equals $\tilde{\Sigma}_{xy}$, and the dashed horizontal line denotes the long-time average of Σ_{xy}. System size: 120×120 sites in all simulations. The finite size [27] causes a small deviation of $\mathcal{C}_s$ from zero in (b).

of $H_k(m)$ has Chern number $\mathcal{C} = -\mathrm{sgn}(m)$ for $0 < |m| < 2$, while $\mathcal{C} = 0$ otherwise. In the following, we will focus on the experimental relevant situation where the topology of $H(m(t))$ changes from trivial to nontrivial as $m(t) = m_i + (m_f - m_i)[1 - e^{-vt}]$ ($t \geq 0$) is ramped from m_i to m_f with velocity v, undergoing a topological transition with an energy gap closing at time $t = t_c$ and momentum $k_c = 0$ [see Fig. 1(a)]. The initial state is assumed to be the insulating ground state of Hamiltonian $H(m_i)$ at half filling, i.e., a topologically trivial state.

To account for the generically mixed states appearing in the open system dynamics, we consider the time-dependent density matrix $\rho(t)$. Assuming the conservation of lattice-translation invariance, $\rho(t)$ factorizes into the components $\rho_k(t) = \frac{1}{2}[1 + \vec{n}_k(t) \cdot \vec{\sigma}]$ at lattice momentum k in the first Brillouin zone (BZ), where $\vec{\sigma}$ denotes the standard Pauli matrices. The vector $\vec{n}_k$ describes the polarization of ρ_k on the Bloch sphere and its length $p_k = |\vec{n}_k|^2 \leq 1$ measures the purity of the state, which has been coined the purity gap [34–37]. For $p_k(t) > 0$, topologically inequivalent states at time t are distinguished by the instantaneous Chern number [38]
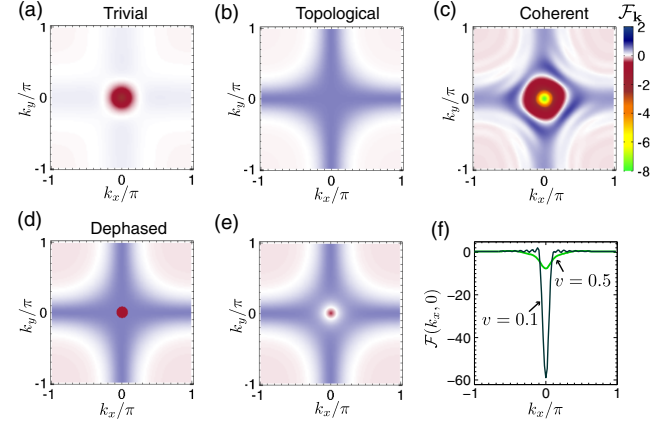
FIG. 2. Berry curvature $\mathcal{F}_k$. (a),(b) Lower band $\mathcal{F}_k$ for (a) the initial Hamiltonian $H(m_i)$ and (b) the final Hamiltonian $H(m_f)$. (c) $\mathcal{F}_k(t)$ for the coherently evolved state at $t > t_c$. (d) Discontinuous $\mathcal{F}_k$ for the dephased steady state. Corresponding weighted curvature $\sqrt{p_k}\mathcal{F}_k$ [the integrand of Eq. (5)] is shown in panel (e). (f) $\mathcal{F}(k_x, 0)$ of the coherently evolved states at $t > t_c$, for $v = 0.1$ and $v = 0.5$, respectively. The simulations are done with a local adaptive method in momentum space resolving system sizes of up to 1795×1795 sites. Ramp velocity $v = 0.5$ (c)–(e), $m_i = -2.5$, $m_f = -1$.

$$\mathcal{C}_s(t) = \frac{1}{2\pi} \int_{\mathrm{BZ}} d^2k \mathcal{F}_k(t), \qquad (2)$$

where the Berry curvature is defined as

$$\mathcal{F}_k = -\frac{1}{2}\hat{n}_k \cdot [(\partial_{k_x}\hat{n}_k) \times (\partial_{k_y}\hat{n}_k)] \qquad (3)$$

with $\hat{n}_k = \vec{n}_k/\sqrt{p_k}$. For $p_k \equiv 1$, $\mathcal{C}_s$ reduces to the standard Chern number of a pure state.

Under coherent evolution, which simply acts as a smooth unitary transformation on $\rho_k(t)$, $\mathcal{C}_s$ is constant in time. Here, while the Hamiltonian (1) enters a topologically nontrivial Chern insulator regime for $t > t_c$, the Chern number of the state $\mathcal{C}_s \equiv 0$ at all times. Beyond coherent dynamics where the state generically becomes mixed with $p_k < 1$, $\mathcal{C}_s$ is protected by the purity gap provided it is finite. If the purity gap closes, i.e., $p_k = 0$ for some k, $\mathcal{C}_s$ becomes undefined.

Nonequilibrium bulk Hall response.—We dynamically probe the nonequilibrium Hall response

$$\Sigma_{xy}(t) = \frac{1}{E_x} \int_{\mathrm{BZ}} d^2k \,\mathrm{Tr}[j_y \rho_k(t)], \qquad (4)$$

where the current j_y in the y direction is generated by a small electric field E_x in the x direction (the 2D system is defined in the xy plane), and we measure conductance in units of e^2/h. To probe the Hall response of the system, we switch on a small homogenous electric field at $t = 0$ as $E_x(t) = E_0[1 - \exp(-t/\tau_e)]$ as generated by a spatially
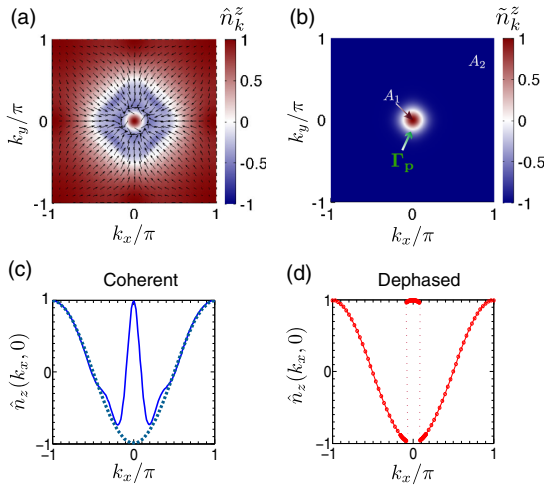
FIG. 3. (a) Bloch vector $\hat{n}_k$ of the coherently evolving state at $t \gg t_c$. Arrows depict the in-plane configuration $(\hat{n}_k^x, \hat{n}_k^y)$, whereas n_k^z is indicated with color. (b) Occupation in the eigenbasis of $H(m_f)$ parametrized by $\tilde{n}_k^z$. Contour Γ_p (closed white curve) defined by $\tilde{n}_k^z = 0$, i.e., at an equal weight superposition of the upper and lower band. (c) $\hat{n}_z(k_x, 0)$ as a smooth function of k_x for $k_y = 0$ for the coherently time-evolved state (blue solid) and the ground state of $H(m_f)$ (blue dashed). (d) $\hat{n}_k^z(k_x, 0)$ for the dephased steady state, which exhibits a discontinuous jump around the purity gap closing point. $m_i = -2.5$, $m_f = -1$, $v = 0.5$ in all plots. $\gamma_k = 0.5$ in (d). The system size is 120×120 sites in all plots.

homogeneous time-dependent vector potential, thus preserving translation invariance. In experiments on cold atoms in optical lattices, such an electric field can be synthetically generated [24]. In our simulations, we choose $\tau_e = 5.0$ and $E_0 = 0.001$, so that the electric field is sufficiently small to have a negligible effect on the state.

To gain intuition for the nonequilibrium nature of the Hall response $\Sigma_{xy}(t)$, we formally interpret $\rho_k(t)$ at every point in time as a canonical thermal density matrix associated with a (fictitious) Hamiltonian $\tilde{H}_k$, i.e., $\rho_k \sim e^{-\tilde{H}_k}$. In this picture, the corresponding equilibrium Hall conductance $\tilde{\Sigma}_{xy}(t)$ as derived [28] from the standard Kubo formula [39] reads

$$\tilde{\Sigma}_{xy}(t) = \frac{1}{2\pi} \int_{\text{BZ}} d^2k \sqrt{p_k(t)} \mathcal{F}_k(t). \tag{5}$$

The deviation of $\tilde{\Sigma}_{xy}(t)$ from the exact value $\Sigma_{xy}(t)$ serves as a measure of how different the nonequilibrium Hall response is from its equilibrium counterpart associated with the same instantaneous state. Note that even if the purity gap p_k closes, $\tilde{\Sigma}_{xy}$ stays well defined by the definition $\sqrt{p_k}\mathcal{F}_k = 0$ for $\sqrt{p_k} = 0$. The intuition behind this continuation is that $\sqrt{p_k} = 0$ represents an infinite temperature state that does not contribute to the Hall conductance.

Quantized Hall response without Chern insulator state.—As a first main result, we show the nonequilibrium Hall response under coherent dynamics where the Chern number $C_s(t)$ is pinned to zero at all times [see Fig. 1(b)]. During the nonadiabatic ramp of $m(t)$ through the gap closing [see Fig. 1(a)], the nonequilibrium population of the eigenstates of $H(m(t))$ is determined by LZ physics [31]: away from k_c where the energy gap is larger than the ramp velocity v at all times, the system stays in the ground state, while close to k_c excitations and coherent superpositions of ground and excited states, respectively, are created. Right at k_c, the excited state is populated with probability 1, thus rendering $\rho(t)$ orthogonal to the ground state of the final Hamiltonian $H(m_f)$. We note that for pure states $\tilde{\Sigma}_{xy} = C_s$. Hence, also $\tilde{\Sigma}_{xy}$ has to stay zero at all times in the thermodynamic limit. By contrast, a significant nonequilibrium Hall response $\Sigma_{xy}(t)$ that shows a strongly oscillatory behavior is found to build up dynamically [see Fig. 1(b)]. In even stronger disagreement with the zero Chern number, its time-averaged value over many oscillation periods approaches asymptotically the quantized value of a Chern band in the limit of small v. Our subsequent analysis regarding the influence of dephasing will give a geometrical picture reconciling of this discrepancy.

Stablization of Hall response by dephasing.—We now show that upon adding classical noise to the dynamics, which induces dephasing, the oscillations of the Hall response Σ_{xy}, as shown in Fig. 1(b) for coherent evolution, damp out. This yields the smooth Hall response plotted in Fig. 1(c)—well captured by $\tilde{\Sigma}_{xy}$ for $t \gg t_c$—which becomes quantized in the slow ramp limit. In the noisy dephasing dynamics the coherent superpositions of excited and ground states of $H_k(m(t))$ are randomized, as described by the master equation for the stochastically averaged density matrix [40–42]

$$\dot{\rho}_k = -i[H_k(m), \rho_k] + \gamma_k[\tilde{\sigma}_k^z \rho_k \tilde{\sigma}_k^z - \rho_k]. \tag{6}$$

Here, $\tilde{\sigma}_k^i(t)$ denote the standard Pauli matrices in the basis of the instantaneous Hamiltonian $H_k(m(t))$ at lattice momentum k. In addition to the Hamiltonian part, Eq. (6) contains a noise-induced pure dephasing term, which preserves the population of the instantaneous eigenstates of $H_k(m(t))$ and thus the average energy, while the relative phase coherence decays at a rate γ_k [43]. The time evolution generated by Eq. (6) does not preserve the purity of the averaged density matrix.

Such a dephasing appears naturally in cold atom experiments with natural or engineered laser noise, where the system parameters become stochastic functions of time. We note that laser fluctuations act as a temporal global noise, which uniformly affects the system. In particular, a fluctuating (global) mass parameter can result from frequency fluctuations or the modulation of the laser light, while (global) fluctuations in the hopping amplitude can arise

from intensity variations. The dephasing terms in the Hamiltonian underlying Eq. (6) are assumed to commute with the system Hamiltonian, as discussed in Ref. [44]. In the limit of fast fluctuations (white noise), the stochastically averaged density matrix obeys the master equation (6).

While the values of both Σ_{xy} and $\tilde{\Sigma}_{xy}$ approach the quantized value reflecting the Chern insulator Hamiltonian in the slow ramp limit $v \ll 1$ [45], the Chern number of the steady state generically becomes undefined due to a purity gap closing. To gain a deeper understanding of this phenomenon, we study below the time-dependent geometric properties of the state described by the stochastically averaged density operator.

Discontinuous Berry curvature and geometric analysis.— In Fig. 2, we compare the Berry curvature [see Eq. (3)] of the dephased and the coherently evolved states to that of the ground states of both $H(m_i)$ and $H(m_f)$. Remarkably, for the dephased state, $\mathcal{F}_k$ exhibits characteristic discontinuities [see Fig. 2(d)] that will allow us to explain the behavior of the Hall response reported above. Note that the experimental observation of the Berry curvature for a system of ultracold atoms has recently been reported [26].

To reveal the effects of dephasing, we represent the density matrix in the eigenbasis of the instantaneous Hamiltonian $H(m(t))$, here denoted by $\rho_k(t) = \frac{1}{2}[1 + \tilde{n}_k(t) \cdot \tilde{\sigma}_k(t)]$. In this basis, the occupation of the upper band at momentum k is simply given by $(1 + \tilde{n}_k^z)/2$, and the dephased steady state is of the form

$$\rho_k^s = \frac{1}{2}(1 + \tilde{n}_k^z \tilde{\sigma}_k^z) = \frac{1}{2}[1 + \tilde{n}_k^z \hat{d}_k(m_f) \cdot \vec{\sigma}], \qquad (7)$$

which is diagonal in the basis of the final Hamiltonian $H(m_f)$ with $\hat{d}_k = \vec{d}_k/|\vec{d}_k|$ and has purity $|\tilde{n}_k^z|^2$. From the coherent LZ dynamics at $t > t_c$, we expect $\tilde{n}_k^z \approx 1$ close to the gap closing momentum k_c and $\tilde{n}_k^z \approx -1$ far away from k_c [see Fig. 3(b)]. Hence, there must be a closed contour Γ_p around k_c in the BZ for $t > t_c$, where the pure system state is an equal weight superposition of the lower and the upper band [$\tilde{n}_k^z(t) = 0$]. On Γ_p, dephasing results in a completely mixed steady state $\rho_k^s = \frac{1}{2}$, implying a purity gap closing in the long-time limit. To visualize this behavior, we show the Berry curvature (see Fig. 2) and the Bloch sphere vector $\hat{n}_k$ of the density matrix ρ_k (see Fig. 3). In the coherent case $\hat{n}_k^z$ stays smooth [see Figs. 3(a) and 3(c)], even though with decreasing v the change of $\hat{n}_k^z$ becomes more and more steep. This gives rise to a sharp peak in the Berry curvature [see Figs. 2(c) and 2(f)], which renders $\mathcal{C}_s$ and $\tilde{\Sigma}_{xy}$ zero, irrespective of v. By contrast, this peak in $\mathcal{F}_k$ is absent in the dephased steady state [see Figs. 2(d) and 2(e)]. Instead, from Eq. (7), we find that

$$\hat{n}_k^s = \frac{\tilde{n}_k^z}{|\tilde{n}_k^z|} \hat{d}_k(m_f) = \text{sgn}(\tilde{n}_k^z)\hat{d}_k(m_f), \qquad (8)$$

which exhibits a discontinuous jump by $2|\hat{d}_k^z(m_f)|$ on Γ_p [see Fig. 3(d)], where $\tilde{n}_k^z$ changes sign. This renders the mixed state Chern number $\mathcal{C}_s$ [see Eq. (2)] undefined, as the Berry curvature is not well defined on Γ_p. However, this discontinuity does not contribute to $\tilde{\Sigma}_{xy}$ as it concurs with the purity gap closing $p_k = 0$. As we see from the asymptotic agreement of the blue and red curves in Fig. 1(c), $\tilde{\Sigma}_{xy}$ provides a good intuition for the real Hall response Σ_{xy} long after t_c.

To compute $\tilde{\Sigma}_{xy}$ [see Eq. (5)], the BZ is decomposed into two patches A_1 and A_2 separated by Γ_p [see Fig. 3(b)]. From Eq. (7), we immediately conclude that $\mathcal{F}_k$ is simply the upper band (lower band) Berry curvature of the final Hamiltonian $H(m_f)$ on A_1 (A_2). The radius of A_1 is proportional to v. Therefore, in the limit of small v, the value of the integral over the BZ is dominated by A_2 and we find to leading order in v [28]

$$\tilde{\Sigma}_{xy} = \mathcal{C} - \frac{1}{2\pi} \frac{v}{|m_f + 2|}, \qquad (9)$$

approaching the value corresponding to the Chern number $\mathcal{C} = 1$ of the lower band of $H(m_f)$. This reconciles the behavior of the Hall response with the underlying mixed state geometry, contrasting the discrepancy between $\mathcal{C}_s$ and Σ_{xy} in the coherent dynamics.

Concluding discussion.—Our present analysis has been based on translation-invariant systems of free fermions. However, our key results are found to be robust in the presence of various imperfections that may occur in real experimental settings. In particular, we have carefully verified that both a trapping potential and weak static disorder only lead to minor quantitative changes in the Hall response [28]. Regarding many-body interactions, the nearly insulating character of the state is expected to limit the influence of multiparticle scattering on the bulk response properties.

In summary, we have shown how the topology of the instantaneous Hamiltonian can manifest itself in the bulk response of a system far from thermal equilibrium, even if its state stays nontopological. In the presence of dephasing we were able to provide a geometric explanation of this phenomenon that goes beyond the well-established framework of topological quantum numbers in closed systems. These results are of immediate relevance for current experiments on synthetic material systems where the preparation of topologically nontrivial Hamiltonians is state of the art while preparing their ground state, or at least a low temperature thermal state, remains an open challenge.

Note added.—Recently, two papers focusing on the non-equilibrium Hall response in the coherent quench dynamics starting from a topologically nontrivial initial state have appeared [46,47].

---

[1] M. Z. Hasan and C. L. Kane, Rev. Mod. Phys. **82**, 3045 (2010).

[2] X. L. Qi and S. C. Zhang, Rev. Mod. Phys. **83**, 1057 (2011).

[3] F. D. M. Haldane, Phys. Rev. Lett. **61**, 2015 (1988).

[4] D. J. Thouless, M. Kohmoto, M. P. Nightingale, and M. den Nijs, Phys. Rev. Lett. **49**, 405 (1982).

[5] B. A. Bernevig and T. L. Hughes, *Topological Insulators and Topological Superconductors* (Princeton University Press, Princeton, NJ, 2013).

[6] N. H. Lindner, G. Refael, and V. Galitski, Nat. Phys. **7**, 490 (2011).

[7] M. S. Foster, M. Dzero, V. Gurarie, and E. A. Yuzbashyan, Phys. Rev. B **88**, 104511 (2013).

[8] M. S. Foster, V. Gurarie, M. Dzero, and E. A. Yuzbashyan, Phys. Rev. Lett. **113**, 076403 (2014).

[9] L. D'Alessio and M. Rigol, Nat. Commun. **6**, 8336 (2015).

[10] M. D. Caio, N. R. Cooper, and M. J. Bhaseen, Phys. Rev. Lett. **115**, 236403 (2015).

[11] J. C. Budich and M. Heyl, Phys. Rev. B **93**, 085416 (2016).

[12] T. Kitagawa, T. Oka, A. Brataas, L. Fu, and E. Demler, Phys. Rev. B **84**, 235108 (2011).

[13] T. Oka and H. Aoki, Phys. Rev. B **79**, 081406(R) (2009).

[14] M. S. Rudner, N. H. Lindner, E. Berg, and M. Levin, Phys. Rev. X **3**, 031005 (2013).

[15] L. E. F. Foa Torres, P. M. Perez-Piskunow, C. A. Balseiro, and G. Usaj, Phys. Rev. Lett. **113**, 266801 (2014).

[16] H. Dehghani, T. Oka, and A. Mitra, Phys. Rev. B **91**, 155422 (2015).

[17] P. Wang, M. Schmitt, and S. Kehrein, Phys. Rev. B **93**, 085134 (2016).

[18] M. Aidelsburger, M. Atala, S. Nascimbéne, S. Trotzky, Y. A. Chen, and I. Bloch, Phys. Rev. Lett. **107**, 255301 (2011).

[19] J. Struck, C. Ölschläger, M. Weinberg, P. Hauke, J. Simonet, A. Eckardt, M. Lewenstein, K. Sengstock, and P. Windpassinger, Phys. Rev. Lett. **108**, 225304 (2012).

[20] M. Atala, M. Aidelsburger, M. Lohse, J. T. Barreiro, B. Paredes, and I. Bloch, Nat. Phys. **10**, 588 (2014).

[21] M. Aidelsburger, M. Atala, M. Lohse, J. T. Barreiro, B. Paredes, and I. Bloch, Phys. Rev. Lett. **111**, 185301 (2013).

[22] H. Miyake, G. A. Siviloglou, C. J. Kennedy, W. C. Burton, and W. Ketterle, Phys. Rev. Lett. **111**, 185302 (2013).

[23] G. Jotzu, M. Messer, R. Desbuquois, M. Lebrat, T. Uehlinger, D. Greif, and T. Esslinger, Nature (London) **515**, 237 (2014).

[24] M. Aidelsburger, M. Lohse, C. Schweizer, M. Atala, J. T. Barreiro, S. Nascimbéne, N. R. Cooper, I. Bloch, and N. Goldman, Nat. Phys. **11**, 162 (2015).

[25] N. Goldman, N. Cooper, and J. Dalibard, arXiv:1507.07805.

[26] N. Fläschner, B. S. Rem, M. Tarnowski, D. Vogel, D.-S. Lühmann, K. Sengstock, and C. Weitenberg, Science **352**, 1091 (2016).

[27] Regarding the relevance of finite sized effects in our simulations, see also the Supplemental Material [28].

[28] See Supplemental Material at http://link.aps.org/supplemental/10.1103/PhysRevLett.117.126803 also, which includes Refs. [29,30], for details.

[29] C. Gardiner and P. Zoller, *Quantum Noise* (Springer, New York, 2004).

[30] A. Griessner, A. J. Daley, S. R. Clark, D. Jaksch, and P. Zoller, New J. Phys. **9**, 44 (2007).

[31] L. D. Landau and E. M. Lifshitz, *Quantum Mechanics* (Pergamon, New York, 1958); C. Zener, Proc. R. Soc. A **137**, 696 (1932).

[32] We note that our analysis can readily be generalized beyond this minimal setting of two-banded models.

[33] X. L. Qi, T. L. Hughes, and S. C. Zhang, Phys. Rev. B **78**, 195424 (2008).

[34] S. Diehl, E. Rico, M. Baranov, and P. Zoller, Nat. Phys. **7**, 971 (2011).

[35] C. E. Bardyn, M. A. Baranov, C. V. Kraus, E. Rico, A. Imamoglu, P. Zoller, and S. Diehl, New J. Phys. **15**, 085001 (2013).

[36] J. C. Budich, P. Zoller, and S. Diehl, Phys. Rev. A **91**, 042117 (2015).

[37] J. C. Budich and S. Diehl, Phys. Rev. B **91**, 165140 (2015).

[38] S. S. Chern, Ann. Math. **47**, 85 (1946).

[39] G. D. Mahan, *Many-Particle Physics* (Springer, New York, 2000).

[40] G. Lindblad, Commun. Math. Phys. **48**, 119 (1976).

[41] C. Gardiner, *Stochastic Methods: A Handbook for the Natural and Social Sciences* (Springer, Berlin, 2010).

[42] Y. Hu, Z. Cai, M. A. Baranov, and P. Zoller, Phys. Rev. B **92**, 165118 (2015).

[43] We have carefully checked that all results reported below are qualitatively unchanged if dephasing is switched on only after the gap closing time t_c.

[44] H. Pichler, J. Schachenmayer, J. Simon, P. Zoller, and A. J. Daley, Phys. Rev. A **86**, 051605(R) (2012).

[45] We note that extremely strong dephasing, i.e., γ_k larger than the energy scale of $H_k(m_f)$, has a detrimental influence on the current, thus suppressing the Hall response Σ_{xy}. In the experimentally natural regime $\gamma_k < 1$, this effect is not visible and can only be observed if very strong dephasing can be engineered.

[46] J. H. Wilson, J. C. W. Song, and G. Refael, arXiv:1603.01621.

[47] M. D. Caio, N. R. Cooper, and M. J. Bahseen, arXiv:1604.04216.